*Inorg. Chem.* **2008**, *47*, 8167−8178

# The Alkylation Mechanism of Zinc-Bound Thiolates Depends upon the Zinc Ligands

**Delphine Picot, Gilles Ohanessian, and Gilles Frison***

*Laboratoire des Mécanismes Réactionnels, Département de Chimie, Ecole Polytechnique and CNRS, 91128 Palaiseau Cedex, France*

Received April 18, 2008

Alkylation of zinc-bound thiolates occurs in both catalytic and structural zinc sites of enzymes. Recent biomimetic studies have led to a controversy as to which mechanism is operative in thiolate alkylation. Building on one of these biomimetic complexes, we have devised a series of models that allow for an appraisal of the roles of charge, ligand nature, and hydrogen bonding to sulfur on reactivity. The reactions of these complexes with methyl iodide, leading to thioethers and zinc iodide complexes, have been examined by density functional theory calculations, in the gas phase as well as in an aqueous solution. In all cases, a $S_N2$ reaction is favored over $\sigma$-bond metathesis. Both the net electronic charge and the hydrogen bond play a significant role in the nucleophilicity of the thiolate. We find that the mechanistic diversity observed experimentally can be explained by the difference in the net charge of the complexes. A dianionic complex follows a dissociative pathway, whereas an associative one is preferred for a neutral system.

## Introduction

Zinc is an essential constituent of more than 300 enzymes and plays both structural and functional roles in these biological systems.[1−5] The active site of the metalloenzymes is typically characterized by a zinc-centered tetrahedral coordination, in which three or four ligands are protein residues for catalytic or structural sites, respectively. Lateral chains of cysteine and histidine, and to a smaller extent of aspartic and glutamic acids, are the most common metal ligands.[6−10] For a functional active site, the fourth ligand is usually a water molecule.

A class of active sites has started to emerge over the past 15 years in which an alkylation reaction occurs on a zinc-bound thiolate.[11,12] The zinc-linked water molecule of a functional active site can indeed be displaced by a thiol, which will then be alkylated after deprotonation. Metal coordination lowers the p$K_a$ of the cysteine thiol to increase the concentration of the reactive thiolate at physiological pH, which functions then as the nucleophile in the alkylation step. This is the case for proteins such as farnesyl transferase[13,14] and geranylgeranyl transferase[15,16] responsible for alkyl group transfers.

More interestingly, enzymes belonging to the structural class, thus lacking a zinc-bound water molecule in the enzyme resting state, are able to undergo the same kind of reactivity. In these cases, alkylation takes place either at a zinc-bound cysteine residue of the protein or at a thiol substrate bonded to zinc after displacement of a ligand of the metal. The first example to be characterized was the DNA repair protein Ada, which possesses a $Cys_4$ zinc center in its N-terminal side. Among the four cysteines of its zinc core,

* To whom correspondence should be addressed. E-mail: gilles.frison@polytechnique.org. + 00 33 (0)1 69 33 48 03.

(1) Vallee, B. L.; Auld, D. S. *Biochemistry* **1990**, *29*, 5647–5659.
(2) Vallee, B. L.; Auld, D. S. *Proc. Natl. Acad. Sci. U.S.A.* **1990**, *87*, 220–224.
(3) Vallee, B. L.; Auld, D. S. *Acc. Chem. Res.* **1993**, *26*, 543–551.
(4) Lipscomb, W. N.; Strater, N. *Chem. Rev.* **1996**, *96*, 2375–2433.
(5) Coleman, J. E. *Curr. Opin. Chem. Biol.* **1998**, *2*, 222–234.
(6) Vallee, B. L.; Auld, D. S. *FEBS Lett.* **1989**, *257*, 138–140.
(7) Karlin, S.; Zhu, Z.-Y. *Proc. Natl. Acad. Sci. U.S.A.* **1997**, *94*, 14231–14236.
(8) Auld, D. S. *Biometals* **2001**, *14*, 271–313.
(9) Patel, K.; Kumar, A.; Durani, S. *Biochim. Biophys. Acta* **2007**, *1774*, 1247–1253.
(10) Tamames, B.; Sousa, S. F.; Tamames, J.; Fernandes, P. A.; Ramos, M. J. *Proteins* **2007**, *69*, 466–475.
(11) Matthews, R. G.; Goulding, C. W. *Curr. Opin. Chem. Biol.* **1997**, *1*, 332–339.
(12) Penner-Hahn, J. *Curr. Opin. Chem. Biol.* **2007**, *11*, 166–171.
(13) Hightower, K. E.; Fierke, C. A. *Curr. Opun. Chem. Biol.* **1999**, *3*, 176–181.
(14) Strickland, C. L.; Weber, P. C. *Curr. Opin. Drug Discovery Dev.* **1999**, *2*, 475–483.
(15) Zhang, F. L.; Casey, P. J. *Biochem. J.* **1996**, *320*, 925–932.
(16) Lane, K. T.; Beese, L. S. *J. Lipid Res.* **2006**, *47*, 681–699.

10.1021/ic800697s CCC: $40.75 
Published on Web 08/20/2008

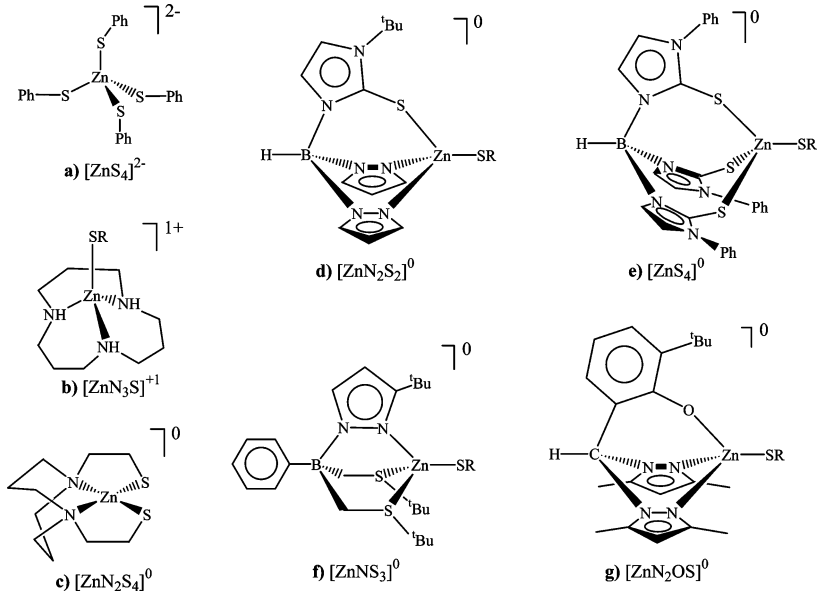


**Figure 1.** Examples of synthetic complexes miming the alkyl transfer activity of protein: (a) refs 28 and 29; (b) refs 49 and 50; (c) ref 51; (d) refs 41 and 45; (e) ref 39; (f) refs 46 and 47; (g) ref 48.

Cys38 is specifically alkylated.[17,18] The methyl group transfer from the phosphotriester DNA backbone is irreversible and, therefore, Ada is considered as a sacrificial agent for DNA repair.[19−21] Other examples include the cobalamin-independent and cobalamin-dependent methionine synthase enzyme family, which methylates homocysteine to produce the amino acid methionine,[22,23] and the two retroviral HIV-1 nucleocapsid protein p7 (Ncp7) zinc fingers, where one of the zinc core cysteine thiolates can be alkylated, leading to inhibition of HIV-1.[24−27]

To study the nature and reactivity of enzymatic cores, biomimetic models have been developed. The first prominent biological models were a series of $[ZnN_2S_2]^0$, $[ZnS_3]^-$, and $[ZnS_4]^{2-}$ complexes[28,29] including the dianionic complex $Zn(SPh)_4^{2-}$ (Figure 1a) used to model the $[Zn(S\text{-}Cys)_4]^{2-}$ active site of the Ada DNA repair protein.

Because of the high tendency of zinc complexes to polymerize,[30,31] most of the complexes developed since then reproduced the thiolate tetrahedral arrangement around the metal with macrocyclic or tripodal ligands with facial binding to the metal and one monodentate ligand. The basic building blocks of tripodal complexes are tris(pyrazolyl)borate[32,33] and tris(mercaptoimidazolyl)borate[34,35] in which the S arms exhibit electronic structures that are intermediate between those of thioketone and the thiolate moiety.[36−38] All of the tripodal arms of these derivatives can be easily mixed to provide the desired number of nitrogen or sulfur ligand donors (Figure 1d,e).[39−45] They may also be replaced by other N, O, or S donor groups to provide tripodal ligand zinc complexes of the desired structures (Figure 1f,g).[46−48] To the best of our knowledge, $Zn(SPh)_4^{2-}$ and $Zn(SPh)_3(ImMe)^-$ (ImMe = methylimidazole) are the only negatively charged inorganic zinc species that have been used so far for biomimetic studies of thiolate alkylation, whereas other zinc thiolate complexes are all neutral (Figure 1c−g) or positively charged (Figure 1b).[49,50]

(17) He, C.; Hus, J. C.; Sun, L. J.; Zhou, P.; Norman, D. P. G.; Dotsch, V.; Wei, H.; Gross, J. D.; Lane, W. S.; Wagner, G.; Verdine, G. L. *Mol. Cell* **2005**, *20*, 117–129.
(18) Takinowaki, H.; Matsuda, Y.; Yoshida, T.; Kobayashi, Y.; Ohkubo, T. *Protein Sci.* **2006**, *15*, 487–497.
(19) Myers, L. C.; Terranova, M. P.; Ferentz, A. E.; Wagner, G.; Verdine, G. L. *Science* **1993**, *261*, 1164–1167.
(20) Ohkubo, T.; Sakashita, H.; Sakuma, T.; Kainosho, M.; Sekiguchi, M.; Morikawa, K. *J. Am. Chem. Soc.* **1994**, *116*, 6035–6036.
(21) Myers, L. C.; Jackow, F.; Verdine, G. L. *J. Biol. Chem.* **1995**, *270*, 6664–6670.
(22) Peariso, K.; Goulding, C. W.; Huang, S.; Matthews, R. G.; Penner-Hahn, J. E. *J. Am. Chem. Soc.* **1998**, *120*, 8410–8416.
(23) Matthews, R. G. *Acc. Chem. Res.* **2001**, *34*, 681–689.
(24) Tummino, P. J.; Scholten, J. D.; Harvey, P. J.; Holler, T. P.; Maloney, L.; Gogliotti, R.; Domagala, J.; Hupe, D. *Proc. Natl. Acad. Sci. U.S.A.* **1996**, *93*, 969–973.
(25) Loo, J. A.; Holler, T. P.; Sanchez, J.; Gogliotti, R.; Maloney, L.; Reily, M. D. *J. Med. Chem.* **1996**, *39*, 4313–4320.
(26) Hathout, Y.; Fabris, D.; Han, M. S.; Sowder, R. C.; Henderson, L. E.; Fenselau, C. *Drug. Metab. Dispos.* **1996**, *24*, 1395–1400.
(27) Maynard, A. T.; Huang, M.; Rice, W. G.; Covell, D. G. *Proc. Natl. Acad. Sci. U.S.A.* **1998**, *95*, 11578−11583.
(28) Wilker, J. J.; Lippard, S. J. *J. Am. Chem. Soc.* **1995**, *117*, 8682–8683.
(29) Wilker, J. J.; Lippard, S. J. *Inorg. Chem.* **1997**, *36*, 969–978.
(30) Watson, A. D.; Rao, C. P.; Dorfman, J. R.; Holm, R. H. *Inorg. Chem.* **1985**, *24*, 2820–2826.
(31) Henkel, G.; Krebs, B. *Chem. Rev.* **2004**, *104*, 801–824.
(32) Parkin, G. Alkyl, Hydride, and Hydroxide Derivatives of the s- and p-Block Elements Supported by Poly(pyrazolyl)borato Ligation: Models for Carbonic Anhydrase, Receptors for Anions, and the Study of Controlled Crystallographic Disorder. In *Advances in Inorganic Chemistry*; Sykes, A. G., Ed.; Academic Press: New York, 1995; Vol. *42*, pp 291−393.
(33) *Scorpionates: The Coordination Chemistry of Polypyrazolylborate Ligands*; Trofimenko, S., Ed.; Imperial College Press: London, 1999.
(34) Garner, M.; Reglinski, J.; Cassidy, I.; Spicer, M. D.; Kennedy, A. R. *Chem. Commun.* **1996**, 1975–1976.
(35) Reglinski, J.; Garner, M.; Cassidy, I. D.; Slavin, P. A.; Spicer, M. D.; Armstrong, D. R. *J. Chem. Soc., Dalton Trans.* **1999**, 2119–2126.
(36) Frison, G.; Sevin, A. *J. Phys. Chem. A* **1999**, *103*, 10998–11003.
(37) Frison, G.; Sevin, A. *J. Chem. Soc., Perkin Trans. 2* **2002**, 1692–1697.
(38) Morlok, M. M.; Docrat, A.; Janak, K. E.; Tanski, J. M.; Parkin, G. *Dalton Trans.* **2004**, 3448–3452.

The development of such biomimetic complexes has been a considerable progress in the study of biological thiolate alkylation. Indeed, this enzymatic reaction supplied by zinc has raised numerous questions about its possible mechanisms and the relative reactivity of the thiolates located in the sphere of influence of zinc, which are difficult to answer based exclusively on enzyme studies.

A first question about enzymatic alkylation concerns the reactivity modulation of the zinc active sites due to the nature of the site itself and of its close environment. The impact of the ligand nature on the reactivity of the zinc-bound thiolate has been studied on scorpionate−zinc thiolate complexes containing diverse atom donors (N, O, and S; Figure 1g).[48] Analysis of kinetic data shows a significant increase of the reaction rate, as the donor atom X in the $[N_2X]^-$ heteroscorpionate ligand is changed from O to N to S. Furthermore, experimental rates of reaction, obtained for a series of $[ZnN_3S]^0$, $[ZnN_2S_2]^0$, $[ZnNS_3]^0$, and $[ZnS_4]^0$ complexes derived from tris(pyrazolyl)- and tris(mercaptoimidazolyl)borate (Figure 1d,e),[45] suggest that the nucleophilicity of the biomimetic complex is proportional to the number of S donors of their ligands. This clearly indicates that thiolate reactivity is dependent upon the nature of the tripodal ligand. Both the nature of the zinc ligands and the electric charge are modified in the $[ZnS_4]^{2-}$, $[ZnS_3N]^-$, and $[ZnS_2N_2]^0$ series synthesized by Wilker and Lippard (Figure 1a),[29] who reported the following kinetic trend of alkylation ability: $Zn(SPh)_4^{2-} > Zn(SPh)_3(MeIm)^- \gg Zn(SPh)_2(MeIm)_2$.

The reactivity of "bare" zinc cores is thus dependent upon their ligands and their charges, but such sites are not found in proteins because they are embedded in a hydrogen-bond network provided by the surrounding biological macromolecule that influences their reactivity.[52]

This is, for example, the case in the HIV-1 nucleocapsid protein p7 (Ncp7) zinc finger. This domain contains two copies of a conserved "retroviral-type" sequence Cys-$X_2$-Cys-$X_4$-His-$X_4$-Cys. The zinc center of its C-terminal side is structurally similar to the one situated in its N-terminal side.[53] However, experimental studies reveal that the reaction is substantially faster for the former.[25,26] Furthermore, calculations[52] indicate that a well-protected $Cys_4$ core could be less reactive than some $Cys_3His$ or $Cys_2His_2$ cores. This is consistent with the finding that the $Cys_3His$ C-terminal Ncp7 core is much more vulnerable to electrophiles than the $Cys_4$ core of GATA-1.[54]

While several active sites can present different reactivities depending on their global environment, it has also been established that two thiolates from the same active site can afford diverse nucleophilicities, according to their individual molecular interactions. N−H···S hydrogen bondings between S atoms and backbone amide groups have been indeed proposed to influence directly the reactivity of the thiolate. This is the case in the Ada DNA repair protein, which is alkylated specifically on Cys38.[18] As an explanation of this selectivity, the X-ray structure shows that the three other zinc thiolate ligands of the enzyme (Cys42, Cys69, and Cys72) are engaged in hydrogen bondings, contrary to Cys38, which lacks potential hydrogen-bond donors.[17] Kinetic studies on inorganic models have been conducted to measure the impact of a hydrogen bond on the thiolate. They showed that zinc thiolate alkylation is markedly slower when the thiolate is involved in a hydrogen bond.[42,47,55−59]

Another question has been raised about the mechanism of the sulfur alkylation, which can, in principle, occur via a manifold of pathways. Three of them have emerged from previous studies, illustrated in Figure 2 with $CH_3I$ as the alkylating agent.[12,60]

In the first one, the dissociative $S_N2$ pathway (path a of Figure 2), the reactants first dissociate to give the reactive species **DISS**. The dissociated thiolate then adds to the alkylating agent $CH_3I$ via an $S_N2$-like transition state (**TS1**) to form the methylated dissociated product. In the other nucleophilic pathway (path b of Figure 2), the alkylation reaction occurs directly between the zinc-bound thiolate (**REACT**) and methyl iodide. The $S_N2$-type transition state **TS2** leads to a zinc-bound thioether (**INT5**), which may dissociate from the metal to give, as in the other pathways, a free thioether and a zinc iodine complex (**PROD**). The third pathway is based on a $\sigma$-bond metathesis reaction (path c of Figure 2). The reactant adds to the electrophile in a


(39) Bridgewater, B. M.; Fillebeen, T.; Friesner, R. A.; Parkin, G. *J. Chem. Soc., Dalton Trans.* **2000**, 4494–4496.
(40) Melnick, J. G.; Docrat, A.; Parkin, G. *Chem. Commun.* **2004**, 2870–2871.
(41) Ji, M.; Benkmil, B.; Vahrenkamp, H. *Inorg. Chem.* **2005**, *44*, 3518–3523.
(42) Ibrahim, M. M.; Seebacher, J.; Steinfeld, G.; Vahrenkamp, H. *Inorg. Chem.* **2005**, *44*, 8531–8538.
(43) Ibrahim, M. M.; He, G.; Seebacher, J.; Benkmil, B.; Vahrenkamp, H. *Eur. J. Inorg. Chem.* **2005**, 4070–4077.
(44) Ibrahim, M. M.; Shu, M.; Vahrenkamp, H. *Eur. J. Inorg. Chem.* **2005**, 1388–1397.
(45) Rombach, M.; Seebacher, J.; Ji, M.; Zhang, G. F.; He, G. S.; Ibrahim, M. M.; Benkmil, B.; Vahrenkamp, H. *Inorg. Chem.* **2006**, *45*, 4571–4575.
(46) Chiou, S. J.; Innocent, J.; Riordan, C. G.; Lam, K. C.; Liable-Sands, L.; Rheingold, A. L. *Inorg. Chem.* **2000**, *39*, 4347–4353.
(47) Chiou, S. J.; Riordan, C. G.; Rheingold, A. L. *Proc. Natl. Acad. Sci. U.S.A.* **2003**, *100*, 3695–3700.
(48) Warthen, C. R.; Hammes, B. S.; Carrano, C. J.; Crans, D. C. *J. Biol. Inorg. Chem.* **2001**, *6*, 82–90.
(49) Notni, J.; Görls, H.; Anders, E. *Eur. J. Inorg. Chem.* **2006**, 1444–1455.
(50) Notni, J.; Gunther, W.; Anders, E. *Eur. J. Inorg. Chem.* **2007**, 985–993.
(51) Grapperhaus, C. A.; Tuntulani, T.; Reibenspies, J. H.; Darensbourg, M. Y. *Inorg. Chem.* **1998**, *37*, 4052–4058.
(52) Maynard, A. T.; Covell, D. G. *J. Am. Chem. Soc.* **2001**, *123*, 1047–1058.
(53) South, T. L.; Blake, P. R.; Hare, D. R.; Summers, M. F. *Biochemistry* **1991**, *30*, 6342–6349.
(54) Huang, M. J.; Maynard, A.; Turpin, J. A.; Graham, L.; Janini, G. M.; Covell, D. G.; Rice, W. G. *J. Med. Chem.* **1998**, *41*, 1371–1381.
(55) Smith, J. N.; Shirin, Z.; Carrano, C. J. *J. Am. Chem. Soc.* **2003**, *125*, 868–869.
(56) Smith, J. N.; Hoffman, J. T.; Shirin, Z.; Carrano, C. J. *Inorg. Chem.* **2005**, *44*, 2012–2017.
(57) Morlok, M. M.; Janak, K. E.; Zhu, G.; Quarless, D. A.; Parkin, G. *J. Am. Chem. Soc.* **2005**, *127*, 14039–14050.
(58) Melnick, J. G.; Zhu, G.; Buccella, D.; Parkin, G. *J. Inorg. Chem.* **2006**, *100*, 1147–1154.
(59) Ibrahim, M. M. *Inorg. Chim. Acta* **2006**, *359*, 4235–4242.
(60) Parkin, G. *Chem. Rev.* **2004**, *104*, 699–767.

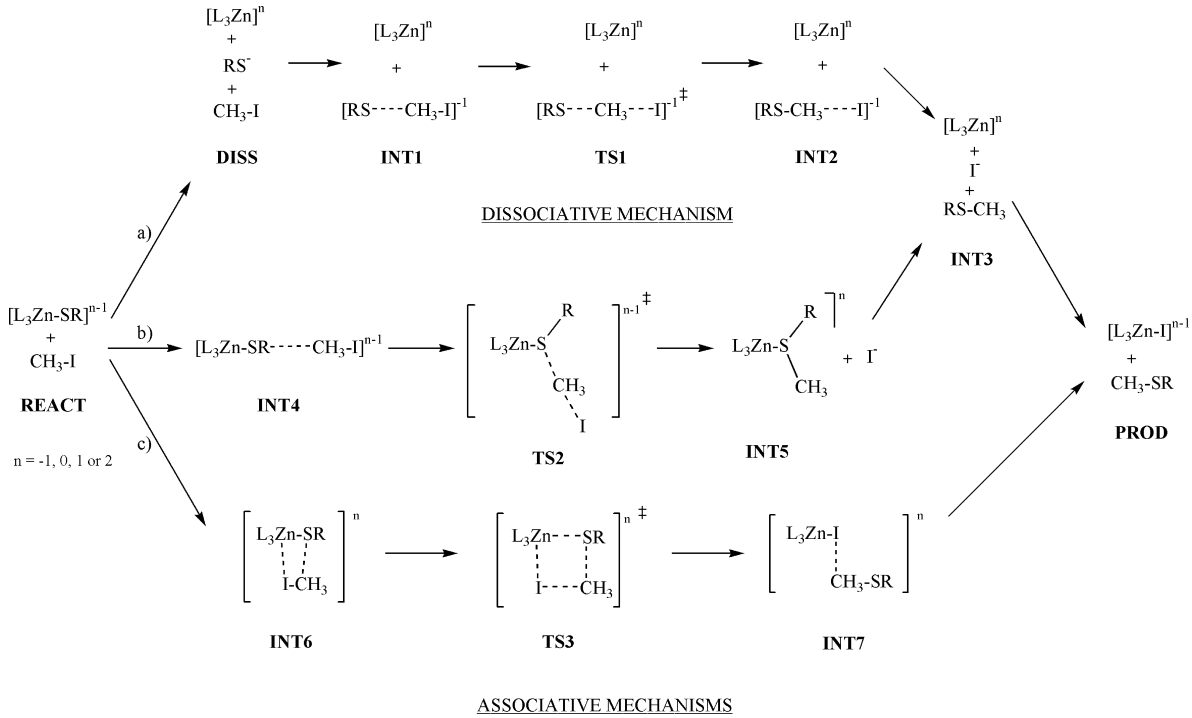


**Figure 2.** Possible mechanistic pathways for the alkylation of a zinc-bound thiolate by methyl iodide.

four-center transition state (**TS3**). Thiolate alkylation and breaking of the zinc thiolate bond occur simultaneously.

The results of numerous experiments on $[ZnN_nS_{4-n}]^0$ or $[ZnN_nS]^+$ complexes (Figure 1) point to an alkylation with an associative mechanism on the basis of second-order kinetics.[45,48,50,57,61,62] Furthermore, the temperature dependence of the alkylation is characterized by a small positive activation enthalpy and a large negative entropy whose values are in the range observed for reactions known to proceed by an associative pathway.[48,57]

Theoretical and experimental mechanistic studies on the farnesyl transferase enzyme or on the Ncp7 zinc finger are in agreement with this mechanism.[13,63−65] The most likely catalytic mechanism of the nucleophilic cysteine reaction with electrophilic reagents involves indeed a zinc-bound thiolate.

To the contrary, Wilker and Lippard report a dissociative alkylation of $Zn(SPh)_4^{2-}$ (Figure 1a).[29] The zinc complex is suggested to undergo appreciable degrees of dissociation before addition to the alkylating agent $(CH_3O)_3PO$ and thus, in the same way, the Ada DNA repair enzyme alkylation proceeds via an initial heterolytic dissociation generating a thiolate, being the active species. This is in agreement with recent kinetic isotope effect studies on a $[ZnS_4]^0$ complex[57] interpreted as indicating a dissociative mechanism, but on the basis of density functional theory (DFT) calculations, the authors cannot exclude thiolate alkylation before dissociation of the ligand.

Until now, there has been no study relating issues about the structure of the zinc complexes, their reactivity, and their alkylation mechanisms. There is, nevertheless, a real need for a link between all of these aspects. This is the objective of this paper, in which we study the impact of structural components of zinc complexes, including hydrogen bonding on a thiolate, on the dissociative vs associative pathway for thiolate alkylation.

## Chemical and Computational Models

**1. Chemical Models.** We need biomimetic models that are appropriate for both structural and mechanistic studies. On the basis of the experimental studies summarized above, we search for a consistent series of zinc complexes in which the ligands, the electric charge, and the availability of hydrogen bonding to thiolate can be varied. In order to delineate the influence of each of these components, these complexes must be relatively rigid,[66] thus four ligand models such as $[Zn(SR)_n(Im)_{4-n}]^{2-n}$ are avoided, but should keep the same steric obstruction of the zinc ion.[50] On the basis of these criteria, we chose the {(pyrazolyl)bis[(methylthio)methyl]hydroborato}zinc complexes **1** and **2**, abbreviated as $[H(pz^H)Bt^{Me}]Zn(SR)$ and depicted in Figure 3, which are $[ZnNS_3]^0$ simplified analogues of zinc complexes of phenyl(3-*tert*-butylpyrazolyl)bis[(*tert*-butylthio)methyl]borate (Figure 1f) that have been synthesized and characterized.[46,47]

**1** and **2** have a $[ZnNS_3]^0$ core, which may be compared to neutral zinc enzyme active sites that include either $[ZnN_2S_2]^0$, with two histidines and two cysteinates bound to zinc, or $[ZnNS_3]^0$ and $[ZnS_4]^0$ with respectively one and two neutral cysteines bound to zinc, as considered in mass spectrometric[67,68] and theoretical[69] studies.

(61) Brand, U.; Rombach, M.; Seebacher, J.; Vahrenkamp, H. *Inorg. Chem.* **2001**, *40*, 6151–6157.
(62) Fox, D. C.; Fiedler, A. T.; Halfen, H. L.; Brunold, T. C.; Halfen, J. A. *J. Am. Chem. Soc.* **2004**, *126*, 7627–7638.
(63) Huang, C. C.; Hightower, K. E.; Fierke, C. A. *Biochemistry* **2000**, *39*, 2593–2602.
(64) Topol, I. A.; Nemukhin, A. V.; Chao, M.; Iyer, L. K.; Tawa, G. J.; Burt, S. K. *J. Am. Chem. Soc.* **2000**, *122*, 7087–7094.
(65) Sousa, S. F.; Fernandes, P. A.; Ramos, M. J. *Proteins* **2007**, *66*, 205–218.
(66) Frison, G.; Ohanessian, G. , submitted for publication.
(67) Fabris, D.; Zaia, J.; Hathout, Y.; Fenselau, C. *J. Am. Chem. Soc.* **1996**, *118*, 12242–12243.

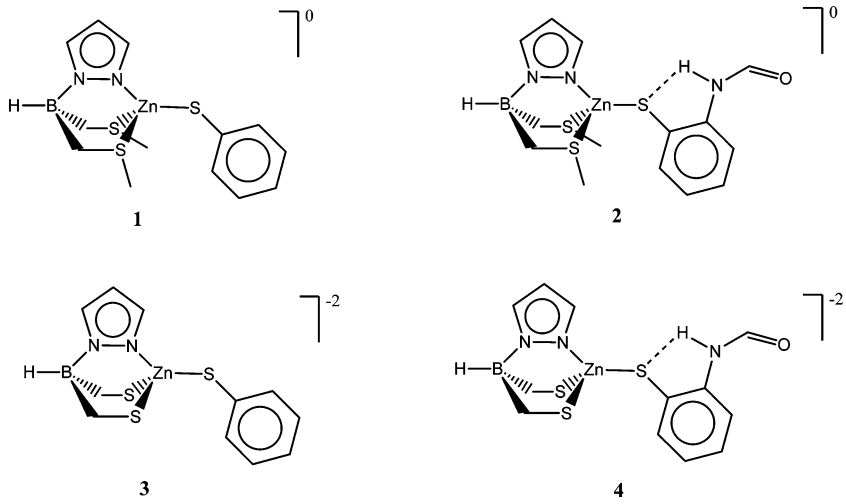


**Figure 3.** Biomimetic zinc complexes studied herein.

Other experimental[70−72] and theoretical[52,73] studies claim that all cysteines are deprotonated when bound to zinc, leading to $[ZnNS_3]^-$ and $[ZnS_4]^{2-}$ cores. In order to study the effect of the ligand charge, we generate complexes **3** and **4**, abbreviated as $[H(pz^H)Bt^{2-}]Zn(SR)$ and $[ZnNS_3]^{2-}$ analogues of **1** and **2**, by removing the sulfur methyls. Furthermore, the electronic richness and its consequence on the reactivity can then be measured effectively by comparing neutral $[ZnNS_3]^0$ complexes **1** and **2** and negatively charged $[ZnNS_3]^{2-}$ complexes **3** and **4**.

The alkylating reagent chosen is methyl iodide, used in many previous experimental studies.[41,45,48,55,57,59] Its addition will be examined exclusively on the aryl thiolate of our models.

**2. Level of Computation.** Calculations were performed with *Gaussian 03*.[74] Geometry optimizations were conducted using the B3LYP method at the 6-31G(d,p) level for the B, N, C, O, S, and H atoms. The contracted Wachters basis [14s9p5d1f/9s5p3d1f] was used to describe the Zn atom.[75] The CRENBL relativistic effective core potential and associated valence basis set were employed to model the I atom.[76] This basis set is referred to as BS1.

Each stationary point has been characterized with frequency analysis and shows the correct number of negative eigenvalues (zero for a local minimum and one for a transition state). All transition states **TS1**−**3** (Figure 2) for all complexes were verified by stepping along the reaction coordinate (intrinsic reaction coordinate calculations) and confirming that they transformed into the reactants/products **INT1** and **-2**, **INT4** and **-5**, and **INT6** and **-7**, respectively (Figure 2). Energies were calculated for the stationary points at the B3LYP level using an extended basis set labeled BS2. It consists of the 6-311+G(2d,2p) for B, N, C, O, S, and H, the extended Wachters basis [15s11p6d2f/10s7p4d2f] for Zn, and the Aug-cc-pVTZ-PP basis set and pseudopotential for I.[77]

The gas-phase Gibbs free energy corresponding to a given reaction was deduced from the equation

$$\Delta G_{gas} = \Delta E_{elec} + \Delta ZPE + \Delta E_T - T\Delta S \qquad (1)$$

with $\Delta E_{elec}$, $\Delta ZPE$, $\Delta E_T$, and $\Delta S$ the differences in the electronic energy, zero-point vibrational energy, thermal energy, and entropy between the products and reactants, respectively.

The solvation free energy of each compound $\Delta G_{solv}$ was determined with the conductor-polarized continuum method (CPCM).[78,79] The CPCM−self-consistent reaction field calculations were carried out at the gas-phase B3LYP/BS1 geometries at the B3LYP level with BS1+ derived from BS1 by the addition of one set of diffuse functions on all atoms except H. The CPCM calculations were performed with tesserae of 0.2 Å$^2$ size, water as the solvent (dielectric constant $\epsilon = 78.39$) and the UAKS cavity.[80]

To calculate the reaction free energy in an aqueous phase ($\Delta G_{water}$), we used the following thermodynamic cycle:

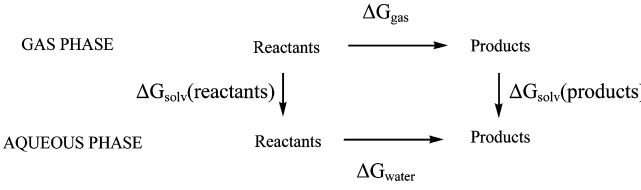


$\Delta G_{gas}$ stands for the gas-phase free energy computed previously and $\Delta G_{solv}(X)$ the free energy necessary for transferring a molecule X from the gas phase to the solvent. The free energy of the reaction in an aqueous phase, $\Delta G_{water}$, can then be deduced from eq 2.

$$\Delta G_{water} = \Delta G_{gas} - \Delta G_{solv}(\text{reactants}) + \Delta G_{solv}(\text{products}) \qquad (2)$$

**3. Evaluation of the Chemical Model and Level of Computation.** Before computational results can be reliably interpreted, the adequacy of the chemical modeling and of the level of computation must be assessed. Several calibration studies have been published recently for the modeling of zinc complexes.[81−87] To this end, we have compared the level of calculation described above, as well as the previously recommended SVWN/6-311++G(d,p),[83] to the available experimental data.[46,47] As can be seen in Table 1 (entries 1, 2, and 5), B3LYP outperforms SVWN for the structure of **1**: Zn−S bond lengths are closer to the crystallographic ones,

(68) Fabris, D.; Hathout, Y.; Fenselau, C. *Inorg. Chem.* **1999**, *38*, 1322–1325.
(69) Simonson, T.; Calimet, N. *Proteins* **2002**, *49*, 37–48.
(70) Chance, M. R.; Sagi, I.; Wirt, M. D.; Frisbie, S. M.; Scheuring, E.; Chen, E.; Bess, J. W.; Henderson, L. E.; Arthur, L. O.; South, T. L.; Perezalvarado, G.; Summers, M. F. *Proc. Natl. Acad. Sci. U.S.A.* **1992**, *89*, 10041–10045.
(71) Dauter, Z.; Wilson, K. S.; Sieker, L. C.; Moulis, J. M.; Meyer, J. *Proc. Natl. Acad. Sci. U.S.A.* **1996**, *93*, 8836–8840.
(72) Clark-Baldwin, K.; Tierney, D. L.; Govindaswamy, N.; Gruff, E. S.; Kim, C.; Berg, J.; Koch, S. A.; Penner-Hahn, J. E. *J. Am. Chem. Soc.* **1998**, *120*, 8401–8409.
(73) Dudev, T.; Lim, C. *J. Am. Chem. Soc.* **2002**, *124*, 6759–6766.

**Table 1.** Main Geometrical Data for the $[ZnNS_3]^0$ Zinc Model[a]

| entry | $R^1$ | $R^2$ | $R^3$ | $R^4$ | method | $Zn-S^1$ | $Zn-S^2$ | $Zn-S^3$ | Zn−N | $N-Zn-S^1-C$ |
|---|---|---|---|---|---|---|---|---|---|---|
| 1 | H | Me | H | H | B3LYP/BS1 | 2.250 | 2.434 | 2.494 | 1.987 | 133.5 |
| 2 | H | Me | H | H | SVWN/6-311++G(d,p) | 2.205 | 2.332 | 2.386 | 1.967 | 143.2 |
| 3 | H | H | H | H | B3LYP/BS1 | 2.238 | 2.471 | 2.561 | 1.972 | 117.6 |
| 4 | H | $^t$Bu | $^t$Bu | H | B3LYP/BS1 | 2.273 | 2.470 | 2.489 | 1.999 | 163.9 |
| 5 | Ph | $^t$Bu | $^t$Bu | H | expt [46] | 2.265 | 2.418 | 2.441 | 2.033 | 171.9 |

[a] See Figure 4 for the labeling of substituents $R^1-R^4$ and sulfur atoms $S^1-S^3$.

with mean deviations of 0.032 and 0.076 Å for B3LYP/BS1 and SVWN/6-311++G(d,p), respectively. This vindicates the choice of B3LYP/BS1 for all geometry optimizations reported herein.

Modeling of the *tert*-butyl on pyrazole and the phenyl on boron by hydrogens, as well as the tripod thiol *tert*-butyls by methyls, does not have a significant impact on the geometry around zinc, except on the relative positions of the tripod and phenylthiolate ligands because their steric repulsions are strongly diminished. This can be seen in Table 1, as measured by the $N-Zn-S^1-C$ dihedral angle, which diminishes from 171.9 to 133.5° (Table 1, entries 1, 4, and 5). On the other hand, modeling of the tripod thiol *tert*-butyls by hydrogens leads to a strong lengthening of one of the Zn−S bonds ($Zn-S^3$; Table 1, entry 3), accentuated by the rotation around the $Zn-S^1$ bond, and is therefore inadequate.

## Results

**1. Structure of Complexes 1−4.** Table 2 reports the structural characteristics of models **1**−**4**. In all cases, the arrangement of the four ligands around zinc is similar, corresponding to a distorted tetrahedron. The steric constraints of the tripodal ligand impose not only a rigid conformation of the ligand around the metal but also acute L−Zn−L (L = tripodal ligand arm) angles as reflected by the measurement of the zinc pyramidality (last column of Table 2), lower than the 328.5° value of the tetrahedral geometry.

The complex **1** possesses two thiols linked to zinc with Zn−S bond lengths of 2.434 and 2.494 Å. Zinc thiolate shows a much smaller bond length of 2.250 Å, reflecting the higher electron density of the thiolate. As already mentioned, these values, as well as the Zn−N bond length of 1.987 Å, are in agreement with the experimental ones.[46] For comparison, recent analyses of the Cambridge Structural Database indicate that the mean Zn−S bond lengths for dialkanethiols and phenylthiolate complexes are 2.55[69] and 2.29 Å,[60] respectively, and that the Zn−N bond lengths are in the range of 2.06−2.19 Å.[69] On this basis, the tripodal ligand seems to tighten the ligand−metal interactions. The $Zn-S^1$ bond length of **1** is slightly shorter than the average Zn−S bond length value of 2.34 Å determined from 22 $ZnCys_4$ binding sites found in the Protein Data Bank, assuming that most or all of the cysteine sulfurs are anionic.[81,83] This could be explained by the effect of the enzyme surrounding (second coordination sphere, enzyme backbone, electrostatic environment,...) that distorts the metal sphere from its ideal geometry, thus weakening the corresponding bonds.

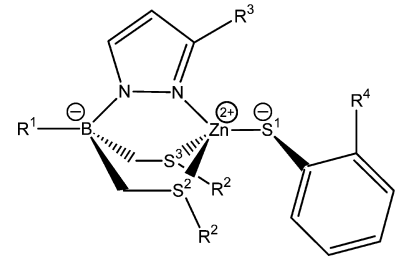


**Figure 4.** Labeling of the $[ZnNS_3]^0$ zinc complexes.

In our designed complex **3**, we transformed the two thiols of **1** into thiolates, leading to reduced Zn−S distances (from 2.434 to 2.324 Å and from 2.494 to 2.320 Å). This large increase in the electron density around Zn leads to a $Zn-S^1$ lengthening of about 0.2 Å in **3** relative to **1**. The $Zn-S^1$ bond is now longer than those of the other two zinc thiolates because the aryl thiolate can delocalize its charge over the phenyl group. This is not possible in the analogous methyl thiolate complex for which the $Zn-S^1$ bond length is computed to be 2.394 Å instead of 2.458 Å in **3** (data not shown). The increased electron density at Zn also leads to a Zn−N lengthening of about 0.16 Å in **3** relative to **1**.

When phenylthiolate is involved in a hydrogen bond as in **2** and **4**, the $Zn-S^1$ bond length slightly increases and the $Zn-S^2$, $Zn-S^3$, and Zn−N lengths slightly decrease

(74) Frisch, M. J.; Trucks, G. W.; Schlegel, H. B.; Scuseria, G. E.; Robb, M. A.; Cheeseman, J. R.; Montgomery, J. A., Jr.; Vreven, T.; Kudin, K. N.; Burant, J. C.; Millam, J. M.; Iyengar, S. S.; Tomasi, J.; Barone, V.; Mennucci, B.; Cossi, M.; Scalmani, G.; Rega, N.; Petersson, G. A.; Nakatsuji, H.; Hada, M.; Ehara, M.; Toyota, K.; Fukuda, R.; Hasegawa, J.; Ishida, M.; Nakajima, T.; Honda, Y.; Kitao, O.; Nakai, H.; Klene, M.; Li, X.; Knox, J. E.; Hratchian, H. P.; Cross, J. B.; Adamo, C.; Jaramillo, J.; Gomperts, R.; Stratmann, R. E.; Yazyev, O.; Austin, A. J.; Cammi, R.; Pomelli, C.; Ochterski, J. W.; Ayala, P. Y.; Morokuma, K.; Voth, G. A.; Salvador, P.; Dannenberg, J. J.; Zakrzewski, V. G.; Dapprich, S.; Daniels, A. D.; Strain, M. C.; Farkas, O.; Malick, D. K.; Rabuck, A. D.; Raghavachari, K.; Foresman, J. B.; Ortiz, J. V.; Cui, Q.; Baboul, A. G.; Clifford, S.; Cioslowski, J.; Stefanov, B. B.; Liu, G.; Liashenko, A.; Piskorz, P.; Komaromi, I.; Martin, R. L.; Fox, D. J.; Keith, T.; Al-Laham, M. A.; Peng, C. Y.; Nanayakkara, A.; Challacombe, M.; Gill, P. M. W.; Johnson, B.; Chen, W.; Wong, M. W.; Gonzalez, C.; Pople, J. A. *Gaussian 03*, revision B.05; Gaussian, Inc.: Pittsburgh, PA, 2003.
(75) Wachters, A. J. *J. Chem. Phys.* **1970**, *52*, 1033–1036.
(76) Lajohn, L. A.; Christiansen, P. A.; Ross, R. B.; Atashroo, T.; Ermler, W. C. *J. Chem. Phys.* **1987**, *87*, 2812–2824.
(77) Peterson, K. A.; Shepler, B. C.; Figgen, D.; Stoll, H. *J. Phys. Chem. A* **2006**, *110*, 13877–13883.
(78) Barone, V.; Cossi, M. *J. Phys. Chem. A* **1998**, *102*, 1995–2001.
(79) Cossi, M.; Rega, N.; Scalmani, G.; Barone, V. *J. Comput. Chem.* **2003**, *24*, 669–681.
(80) Takano, Y.; Houk, K. N. *J. Chem. Theory Comput.* **2005**, *1*, 70–77.
(81) Topol, I. A.; Casas-Finet, J. R.; Gussio, R.; Burt, S. K.; Erickson, J. W. *THEOCHEM* **1998**, *423*, 13–28.
(82) Diaz, N.; Suarez, D.; Merz, K. M., Jr *Chem. Phys. Lett.* **2000**, *326*, 288–292.
(83) Dudev, T.; Lim, C. *J. Phys. Chem. B* **2001**, *105*, 10709–10714.
(84) Sousa, S. F.; Fernandes, P. A.; Ramos, M. J. *J. Chem. Phys. B* **2007**, *111*, 9146–9152.
(85) Frison, G.; Ohanessian, G. *J. Comput. Chem.* **2008**, *29*, 416–433.
(86) Rayon, V. M.; Valdes, H.; Diaz, N.; Suarez, D. *J. Chem. Theory Comput.* **2008**, *4*, 243–256.
(87) Amin, E. A.; Truhlar, D. G. *J. Chem. Theory Comput.* **2008**, *4*, 75–85.

**Table 2.** Main Geometrical Parameters of **1**−**4** (Bond Length in Å and Bond Angle in deg)

| complex | Zn−S$^1$ | Zn−S$^2$ | Zn−S$^3$ | Zn−N | S···HN$^a$ | $\Sigma$(L−Zn−L)$_{tripod}$$^b$ |
|---|---|---|---|---|---|---|
| **1**$^c$ | 2.250 (2.265) | 2.434 (2.418) | 2.494 (2.441) | 1.987 (2.033) | | 286.8 (286.1) |
| **2**$^d$ | 2.262 (2.260) | 2.423 (2.384) | 2.490 (2.410) | 1.984 (2.015) | 2.991 (2.936) | 288.2 (288.6) |
| **3** | 2.458 | 2.324 | 2.320 | 2.141 | | 309.8 |
| **4** | 2.496 | 2.309 | 2.309 | 2.129 | 2.946 | 313.1 |

$^a$ Distance between S$^1$ and N of the intramolecular hydrogen bond. $^b$ Sum of the N−Zn−S$^2$, N−Zn−S$^3$, and S$^2$−Zn−S$^3$ angles. $^c$ Experimental X-ray data[46] in parentheses. $^d$ Experimental X-ray data[47] in parentheses.

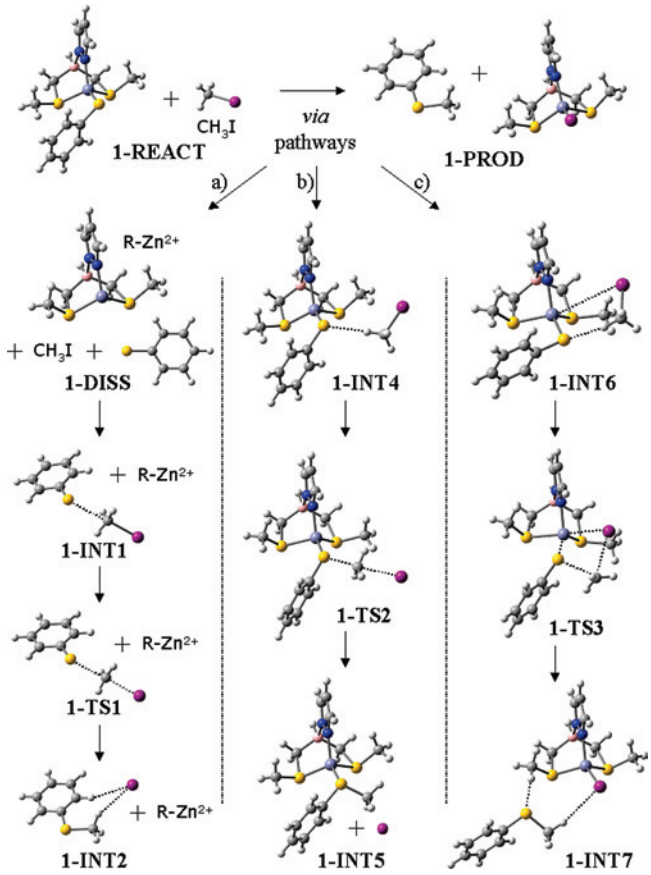


**Figure 5.** Geometrical structures along the reaction paths depicted in Figure 2 for complex **1**. Color code: yellow, sulfur; blue, nitrogen; gray, carbon; white, hydrogen; purple, iodine; pink, boron; light blue, zinc.

concomitantly. This effect is almost insignificant in **2** versus **1**; however, it is larger in **4** versus **3**, to the extent that the Zn−S$^1$ length in **4** is more typical of a thiol than a thiolate. This may have a significant influence on the thiolate nucleophilicity.

The larger effect of hydrogen bonding in **4** versus **2** may be linked to the longer Zn−S$^1$ bond in **3** versus **1**: the thiolate electrons are less involved in bonding to Zn in **3** and, therefore, more available. It is also reflected in the hydrogen bond length, which is much smaller in **4** (2.289 Å) than in **2** (2.378 Å).

**2. Reaction Mechanisms of Complex 1.** Three alkylation mechanisms have been studied as represented in Figure 2: the $S_N2$-type dissociative mechanism (path a), the $S_N2$-type associative mechanism (path b), and the four-center associative one (path c). The optimized structures for all of these pathways for complex **1** are displayed in Figure 5.

The alkylation reaction is exothermic overall with a free-energy release of −17.7 kcal/mol (Table 3). This corresponds to the methylation of the thiolate ligand and its detachment from the boratozinc complex. In the final products, which is the global minimum on the calculated potential free-energy surface, the I ion is complexed by the tripodal-ligated metal cation.

It is immediately evident from the first column of Table 3 that the dissociative pathway a is the least favorable. This is expected because it involves the dissociation of **1** into a $PhS^-$ and tripod zinc cation ion pair, a highly unfavorable process in the gas phase. How much this is modified by solvation will be described in the next section, yet the order remains unchanged.

We first compare the two dissociative (path a) and associative (path b) nucleophilic displacement mechanisms. In the dissociative pathway, the nucleophile is the uncoordinated phenylthiolate **1-DISS** (Figure 5). It is expected to be more reactive than the zinc-bound thiolate **1-REACT** (Figure 5), which is the nucleophile in the associative $S_N2$ reaction. Indeed, a free-energy barrier of 32.3 kcal/mol is associated with the transition state **1-TS2** from the zinc-bound thiolate **1-REACT**, whereas only 1.8 kcal/mol is required from the dissociated nucleophile **1-DISS** to **1-TS1**.

This difference of reactivity is also visible on the geometrical parameters along both reaction paths (Figure 6a,b). Because of the high reactivity of bare thiophenolate, **1-TS1** corresponds to an early transition state with long S···MeI (2.695 vs 1.821 Å in Ph−S−Me) and short Me···I (2.556 vs 2.188 Å in $CH_3I$) bonds. On the contrary, the coordination of the thiophenolate to a zinc cationic fragment in **1-REACT** induces a lower reactivity, as illustrated by the late transition state **1-TS2** with short S···MeI (2.216 Å) and long Me···I (2.895 Å) bonds.

The third pathway (path c) is very different because two bonds (Zn−S and Me–I) are broken and two bonds (S–Me and Zn−I) are created at the same time. **1-TS3** (Figure 5), the transition state along this $\sigma$-bond metathesis reaction, requires 54.4 kcal/mol to be reached, which is about 20 kcal/mol more than the energy needed for **1-TS2** (Table 3). This high energy barrier has already been observed for four-center transition states including an alkyl group at the $\beta$ position with respect to the metal center.[88] Consequently, the $\sigma$-bond metathesis reaction is less favored than the $S_N2$-type associative pathway in the gas phase.

**3. Solvation Effects on Complex 1.** The free energies in an aqueous solution, at the gas-phase geometries, are given for complex **1** in the second column of Table 3. As expected, cationic ($R-Zn^{2+}$ along path a) and anionic ($PhS^-$ in **1-DISS** and $I^-$ in **1-INT5**) species are more strongly solvated than neutral compounds. Compared to

(88) Perrin, L.; Eisenstein, O.; Maron, L. *New J. Chem.* **2007**, *31*, 549–555.

**Table 3.** Relative $\Delta G_{gas}$ and $\Delta G_{water}$ in kcal/mol Calculated at the B3LYP/BS2//B3LYP/BS1 Level Using the CPCM Solvation Model at the B3LYP/BS1+//B3LYP/BS1 Level

| | 1 | | 2 | | 3 | | 4 | |
|---|---|---|---|---|---|---|---|---|
| | $\Delta G_{gas}$ | $\Delta G_{water}$ | $\Delta G_{gas}$ | $\Delta G_{water}$ | $\Delta G_{gas}$ | $\Delta G_{water}$ | $\Delta G_{gas}$ | $\Delta G_{water}$ |
| **REACT** | 0.0 | 0.0 | 0.0 | 0.0 | 0.0 | 0.0 | 0.0 | 0.0 |
| | | | | Pathway a | | | | |
| **DISS** | 128.9 | 23.0 | 116.5 | 19.1 | −38.5 | 2.4 | −40.0 | −0.1 |
| **INT1** | 128.0 | 35.3 | 117.0 | 30.3 | −39.5 | 14.6 | −39.5 | 11.2 |
| **TS1** | 130.7 | 40.9 | 123.3 | 39.7 | −36.7 | 20.3 | −33.2 | 20.6 |
| **INT2** | 105.5 | 7.4 | 101.8 | 11.1 | −61.9 | −13.2 | −54.7 | −8.0 |
| **INT3** | 107.4 | −7.5 | 108.9 | −6.2 | −60.0 | −28.2 | −47.6 | −25.3 |
| | | | | Pathway b | | | | |
| **INT4** | 4.2 | 10.9 | 6.3 | 10.9 | | | | |
| **TS2** | 32.3 | 26.5 | 34.8 | 26.9 | 4.8 | 23.2 | 8.6 | 25.0 |
| **INT5** | 87.5 | −6.1 | 94.4 | −2.4 | −53.6 | −14.1 | −43.6 | −11.0 |
| | | | | Pathway c | | | | |
| **INT6** | 6.9 | 12.4 | 6.6 | 14.0 | | | | |
| **TS3** | 54.4 | 56.4 | 55.5 | 57.3 | | | | |
| **INT7** | −11.4 | −8.4 | −10.2 | −7.5 | | | | |
| **PROD** | −17.7 | −20.7 | −16.3 | −19.3 | −17.4 | −22.3 | −5.0 | −19.4 |

**1-REACT**, this leads to their greater stabilization in solution than in the gas phase.

Solvation induces indeed the reduction of the dissociation free energy of thiophenolate from the zinc complex by more than 100 kcal/mol. Consequently, the free-energy barrier to reach **1-TS1** from the reactants **1-REACT** is considerably reduced from 130.7 to 40.9 kcal/mol. We note, however, that the solvation of $PhS^-$ reduces its reactivity, as shown by the increased activation barrier to reach **1-TS1** from **1-DISS** (+17.9 vs +1.8 kcal/mol in the gas phase). Such dramatic solvation effects on the potential energy profile of pathway a are likely to have some impact on the optimized geometries. It is, however, unlikely that such an effect would lead to a change of the most favorable mechanism. Indeed, the difference between the rate-limiting transition states for pathways a and b is 14.4 kcal/mol (see Table 3 and the discussion below).

On the contrary, solvation induces a greater $S_N2$ reactivity of the zinc-bound phenylthiolate. The activation barrier to reach **1-TS2** from **1-REACT** is indeed diminished from 32.3 kcal/mol in the gas phase to 26.5 kcal/mol in solution. This may be explained by the transient formation in the $S_N2$ associative pathway of two charged species (**1-INT5**) before disruption of the Zn−S(aryl) bond. The associated transition state **1-TS2** has thus small apparent electronic charges and would therefore be more stabilized by the solvent than the neutral reactants.

The effect of water on the relative free energy of **1-TS3** is only 2 kcal/mol because $\sigma$-bond metathesis does not lead to charge separation. Consequently, the energy gap between both associative mechanisms is accentuated by solvent effects and the four-center transition state is the least favored mechanism. The $S_N2$ associative reaction is thus, by far, the most favored alkylation mechanism in water because **1-TS2** lies 29.9 and 14.4 kcal/mol below **1-TS3** and **1-TS1**, respectively.

**4. Influence of Zinc Ligands.** The free energies in the gas phase and in a water solution for the three alkylation mechanisms of complexes **2**−**4** are indicated in Table 3. We first describe the influence of the zinc complex moiety on the potential energy surface by comparing **3** to **1** (and **4** to **2**). In the following section, we will look at the influence of the hydrogen bond on the S atom by comparing **2** to **1** (and **4** to **3**).

The $S_N2$ dissociative mechanism (path a) is the same for **1** and **3**, with the exception of the first step, where the Zn−S(aryl) bond is broken. This dissociative step is exothermic from **3-REACT** in the gas phase because of

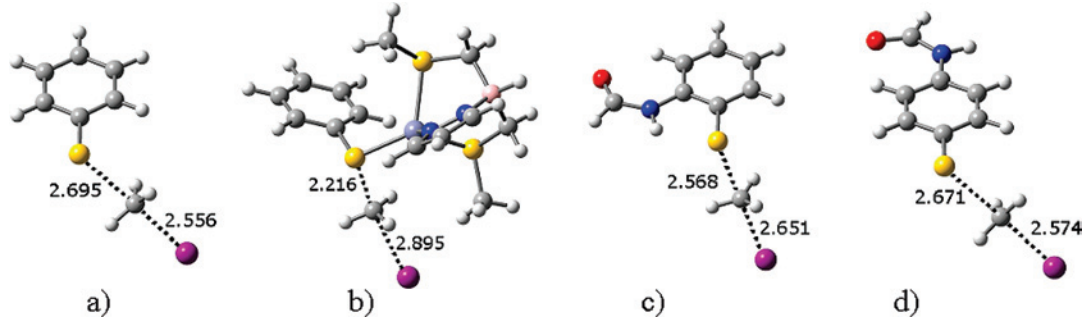


**Figure 6.** Transition-state structures for the $S_N2$ reaction of $CH_3I$ with various phenylthiolates in the gas phase: (a) thiophenolate (**1-TS1**); (b) thiophenolate bound to the $[H(pz^H)Bt^{Me}]Zn$ complex (**1-TS2**); (c) *o*-NHC(O)H-thiophenolate (**2-TS1**); (d) *p*-NHC(O)H-thiophenolate. Color code: yellow, sulfur; red, oxygen; blue, nitrogen; gray, carbon; white, hydrogen; purple, iodine; pink, boron; light blue, zinc.

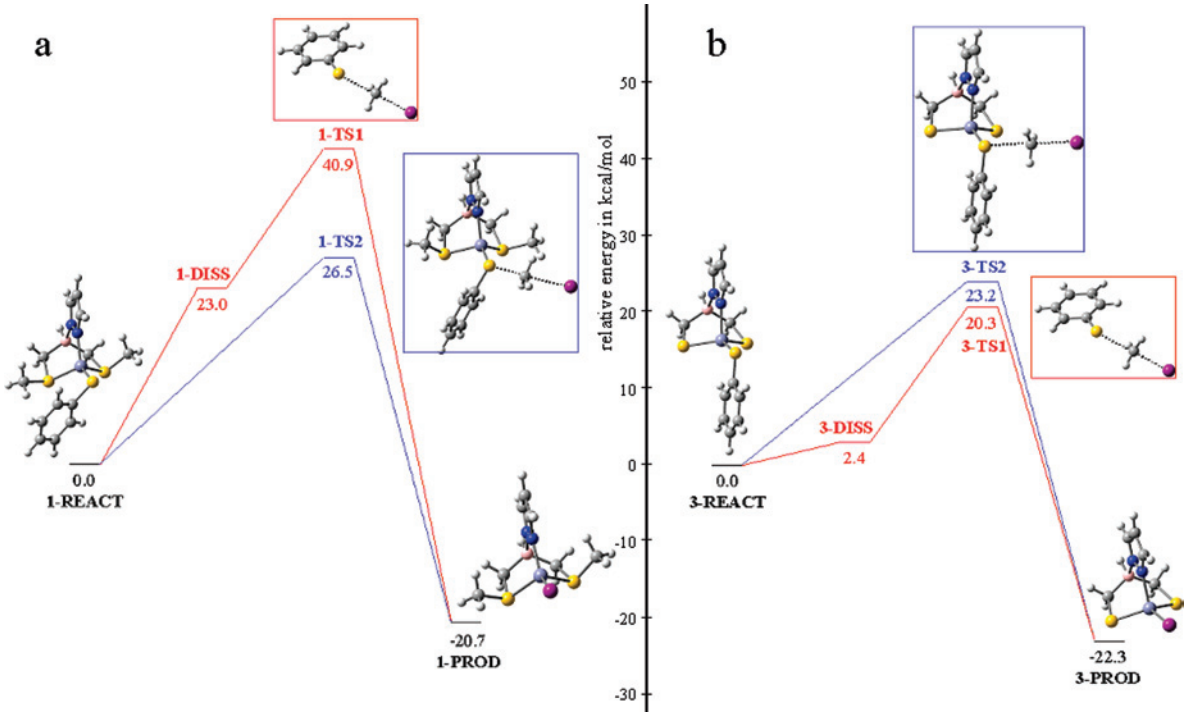


**Figure 7.** Free-energy profiles in a water solution along the dissociative (red) and associative (blue) $S_N2$ pathways for the reaction of MeI with complex **1** (a) and complex **3** (b).

favorable charge−charge separation.[89] As shown previously, this repulsive coulomb effect is visible on the longer Zn−S(aryl) bond length in **3** (2.458 Å) than in **1** (2.250 Å). Inclusion of solvent effects greatly reduces this repulsive interaction, leading to a small positive free dissociation energy of 2.4 kcal/mol. Consequently, an overall free-energy barrier of 20.3 kcal/mol for path a relative to **3-REACT** is computed, much smaller than the 40.9 kcal/mol value obtained from **1-REACT**.

The negative charge of **3-REACT** induces a more pronounced nucleophilic reactivity compared to **1-REACT**. Indeed, **3-TS2** is located only 4.8 kcal/mol higher than the reactants in the gas phase, compared to the 32.3 kcal/mol value obtained for complex **1**. As for the dissociated phenylthiolate (vide supra), inclusion of the solvent effect reduces the reactivity of the anionic complex **3**, increasing the free-energy barrier of path b up to 23.2 kcal/mol, much closer to the value for **1**.

We did not succeed in finding **3-TS3** and **4-TS3** on the potential energy surface. Indeed, any attempt at a four-center transition state leads to the re-formation of $CH_3I$. This may be explained by the very low Lewis acidity of Zn in **3** and **4**, as reflected by the long Zn−ligand bonds (vide supra), due to the two anionic charges of the complexes. We thus advance the hypothesis that path c cannot be followed for electronically rich complexes such as **3** and **4**. In order to confirm the influence of the electronic charge around zinc on the metathesis reactivity, we decide to study the $\sigma$-bond mechanism of a cationic zinc complex. For this purpose, we change the (pyrazolyl)bis[(methylthio)methyl]hydroborato ligand of **1** to the (pyrazolyl)bis[(methylthio)methyl]methane ligand, leading to the new complex $\mathbf{1}^{C}$. As expected, $\mathbf{1}^{C}$**-TS3** is more easily reachable than **1-TS3**, with gas- and water-phase free-energy barriers of respectively 44.9 and 51.1 kcal/mol compared to respectively the 54.4 and 56.4 kcal/mol values for **1-TS3**. However, the $S_N2$ associative mechanism remains preferred for $\mathbf{1}^{C}$ with free-energy barriers of 41.6 and 29.6 kcal/mol in the gas phase and in solution, respectively (data not shown). In nonpolar solvents or buried enzyme sites, it is conceivable that the $\sigma$-bond metathesis be the most favorable in other cases because the difference in free energy between $\mathbf{1}^{C}$**-TS3** and $\mathbf{1}^{C}$**-TS2** is small.

Our results indicate that, contrary to **1** for which the $S_N2$ associative pathway b is much more favorable, the $S_N2$ dissociative pathway a is preferred for **3**, as illustrated in Figure 7. Furthermore, they show that complex **3** will be more easily alkylated than complex **1** because of the lower free energy of **3-TS1** (20.3 kcal/mol) compared to **1-TS2** (26.5 kcal/mol). This is in agreement with experimental results indicating that dianionic zinc biomimetic complexes are more reactive than neutral ones.[28,29] A comparison between **2** and **4** leads to the same conclusion.

**5. Influence of the Hydrogen Bond.** Complex **2** differs from its analogue **1** only by the presence of hydrogen bonding on the phenylthiolate ligand. This has little effect on the dissociated intermediates, which remain high in free energy (116.5 and 19.1 kcal/mol in the gas phase and in water, respectively). The small decrease observed in comparison with **1** is due to a weaker zinc−thiolate interaction in **2**. The Zn−S(aryl) bond length is indeed slightly longer when there is a hydrogen bond on the thiolate (2.262 Å in **2** instead of 2.250 Å in **1**; Table 2).

The effect of the hydrogen bond is marked on the transition state **2-TS1**. Because of the lower dissociation free energy, it is located below **1-TS1**, relative to the reactant complexes, both in the gas phase and in solution. However, the free-

energy barrier of the $S_N2$ step is higher from **2-DISS** (6.8 and 20.6 kcal/mol in the gas phase and in water, respectively) than from **1-DISS** (1.8 and 17.9 kcal/mol, respectively). Participation of the thiolate in a hydrogen bond reduces its nucleophilicity, as was already shown by the kinetics of biomimetic complexes.[47,55,56] The geometries of both transition states **1-TS1** and **2-TS1** illustrate this difference of reactivity between the thiolates (Figure 6a,c). Indeed, **2-TS1** is a later transition state than **1-TS1**, as measured by the shorter S···$CH_3$ (2.568 vs 2.695 Å) and the longer $CH_3$···I (2.651 vs 2.556 Å) distances.

It should be noted that the difference between **1-TS1** and **2-TS1** is not exclusively due to the van der Waals hydrogen-bond interaction.[47] Indeed, a small part of the difference may be due to an inductive or conjugative effect through the phenyl ring. This can be checked by comparing *o*- and *p*-NHC(O)H-thiophenolates because there can be no hydrogen bonding in the latter. The structure of the transition state for the $S_N2$ reaction of $CH_3I$ with *p*-NHC(O)H-thiophenolate is shown in Figure 6d. Its geometrical parameters are intermediate between those of **1-TS1** and **2-TS1** but clearly closer to the former. The associated activation barriers are 3.4 and 18.4 kcal/mol in the gas phase and in water, respectively, which confirm its greater proximity to **1-TS1** than to **2-TS1** (data not shown).

The impact of this hydrogen bonding is less marked but still present for the associative pathways b and c. As in path a, the hydrogen bond decreases the reactivity of the thiolate, leading to higher **2-TS2** and **2-TS3** compared to **1-TS2** and **1-TS3**, respectively, relative to the corresponding reactants. A comparison of the potential free-energy surface from **3-REACT** and from **4-REACT** shows the same results.

These changes in the activation barrier values remain small, however, compared to the differences between the three pathways. Consequently, the $S_N2$ associative path b is the lower energy path from **2-REACT** as from **1-REACT**. The reactivities of **2-REACT** and **4-REACT** are, nevertheless, reduced compared to **1-REACT** and **3-REACT**, respectively, thus showing that, in good adequacy with the experimental results,[47,55,56] a thiolate interacting through a hydrogen bond with an amide is less susceptible to alkylation.

## Discussion

**On the Reactivity of the Zinc Site.** Model complexes have been previously used to determine second-order rate constants of thiolate alkylation. The first study demonstrates a decline of the reactivity from $Zn(SPh)_4^{2-}$ to $Zn(SPh)_3(ImMe)^-$ and $Zn(SPh)_2(ImMe)_2$.[28] This points out the influence of the nature of the zinc ligand and/or of the charge of the complex. Later studies on the thiolate alkylation reactivity of $ZnL_n(SR)$ complexes focus (i) on the nature of the $L_n$ zinc ligand, by varying the zinc-bound atoms (S vs N vs O),[45,48] the number of zinc-bound atoms,[50] or the steric requirement,[42,45,50,58] or (ii) on the nature of the R substituent,[41,42,45,48] or the presence of an intramolecular hydrogen bond in the SR moiety.[47,55,56] Particularly, the rate of alkylation has been shown to increase along the $N_3$, $N_2S$, $NS_2$, and $S_3$ series of ligands $L_n$. It should, however, be noted that, in all of these cases, the comparison of the reactivity is made between complexes bearing the same electronic charge. This situation does not fit the zinc enzyme active sites where N and S ligands are the neutral histidine and the anionic cysteine side chain, respectively, even if the possible protonation of the cysteine side chain is still a matter of debate.[67,68] In this study, we examine the influence both of the charge of the complex and of an intramolecular hydrogen bond in the SR moiety.

Our results show that it is possible to greatly modulate the nucleophilic reactivity of a $ZnNS_3$ complex by changing its global charge. The more negative a zinc site is, the more reactive it is. This is consistent with a previous study on zinc active sites indicating that $[Zn(Cys)_4]^{2-}$ anionic cores are more susceptible to alkylation than the singly charged $[Zn(Cys)_3(His)]^-$ and the neutral $[Zn(Cys)_2(His)_2]$.[52] This also means that the greater reactivity of $Zn(SPh)_4^{2-}$ compared to that of $Zn(SPh)_3(ImMe)^-$ and $Zn(SPh)_2(ImMe)_2$[28] is not exclusively due to the change in the nature of the zinc-bound atoms, from the $ZnS_4$ core to $ZnS_3N$ and $ZnS_2N_2$,[45] but is also a consequence of its greater electronic charge.

Our statement covers two different aspects. First, a more negative environment induces a greater nucleophilicity of the zinc-bound thiolate, as illustrated by the lower free-energy barrier to reach **3-TS2** compared to the corresponding value for **1-TS2** (Table 3). This is observed in a water solution (23.2 and 26.5 kcal/mol, respectively) and, to a larger extent, in the gas phase (4.8 and 32.3 kcal/mol, respectively), illustrating the trend in solvents that are less polar than water, like toluene[47] or chloroform[45] used in some biomimetic studies or in buried enzymatic active sites.

Second, the Zn−S bond is more easily broken in a $[ZnNS_3]^{2-}$ site than in a $[ZnNS_3]^0$ one, leading readily to the more reactive free thiolate (vide infra). Furthermore, thiolate dissociation from **1** is clearly easier in water, with a dissociation energy of 23.0 kcal/mol, than in the gas phase (128.9 kcal/mol). This is in agreement with the experimental observation of thiolate dissociation in $Zn(SPh)_4^{2-}$,[29] whereas there is no thiolate exchange in nonpolar media for $[ZnN_2S_2]^0$ and $[ZnN_3S]^0$ complexes.[61,90] Moreover, changing from nonpolar to polar media leads to possible fast thiolate ligand exchange between neutral zinc cores.[90] It should, however, be noted that thiolate exchange does not necessarily indicate dissociated thiolate because other mechanisms through bridging thiolate complexes may be responsible for the exchange.[58]

A comparison of the nucleophilic reactivity of free and zinc-bound thiolates is in favor of the former, in agreement with experimental results.[28] Indeed, even compared to the dianionic complex **3**, for which $S_N2$ free-energy barriers of 4.8 and 23.2 kcal/mol are obtained in the gas phase and in water, respectively, $PhS^-$ is more nucleophilic, with corresponding free-energy barriers of 1.8 and 17.9 kcal/mol, respectively. This means that the zinc cation in the anionic

(89) Picot, D.; Ohanessian, G.; Frison, G., in preparation.

(90) Seebacher, J.; Ji, M.; Vahrenkamp, H. *Eur. J. Inorg. Chem.* **2004**, 409–417.

$[H(pz^H)Bt^{2-}]Zn$ core keeps some Lewis acidity and thus kinetically stabilizes the zinc-bound thiolate. We postulate that the same applies to the $[Zn(Cys)_4]^{2-}$ electronically rich active sites of enzymes like the DNA repair protein Ada.

Our computational results are in agreement with several experimental studies suggesting that the reactivity of a thiolate is modulated by the presence of a hydrogen bond.[47,55−59] The influence of the hydrogen bond is similar for all thiolates studied here, with an increase of about 4 kcal/mol of the free energy necessary to reach the corresponding $S_N2$ transition state. This may be related to the magnitude of the N−H···S bond.[57] Indeed, the N···S distance is 2.991, 2.946, and 2.951 Å in **2**, **4**, and *o*-NHC(O)H-thiophenolate, respectively, indicative of a similar hydrogen-bond strength.

Complexes **1** and **4** allow one to compare the influence of the charge and of the hydrogen bond. In the gas phase, the total electronic charge is the dominant factor, as illustrated by the lower free-energy barrier to reach **4-TS2** (8.6 kcal/mol) compared to the value for **1-TS2** (32.3 kcal/mol). By contrast, in water, the electronic charge and hydrogen bond influence the nucleophilicity to approximately the same amount. Indeed, a similar free-energy barrier is needed to reach the transition state **TS2** from the neutral complex without hydrogen bond **1** and from the dianionic complex with hydrogen bond **4**. We may postulate that in nonpolar media or in a buried enzyme active site the situation will be intermediate with a weak predominance of the effect of the total electronic charge. Thus, most of the $[Zn(Cys)_4]^{2-}$ enzyme active sites show greater reactivity than $[Zn(Cys)_3(His)]^-$ and $[Zn(Cys)_2(His)_2]^0$ cores, but some exceptions should probably occur as a result of hydrogen-bond networks around the active site. This nicely reflects the predicted rank of zinc finger reactivities evaluated according to protein packing and electrostatic screening of their zinc core.[52] Indeed, in most cases, these properties are similar for $[Zn(Cys)_4]^{2-}$, $[Zn(Cys)_3(His)]^-$, and $[Zn(Cys)_2(His)_2]^0$ cores, reflecting the greater reactivity of the most negatively charged site. However, in some cases, such as the active site of GATA-1, an important steric and electrostatic screening of the $[Zn(Cys)_4]^{2-}$ core is observed compared to that of the $[Zn(Cys)_3(His)]^-$ core of the C-terminal HIV-1 NCp7 zinc finger, in agreement with its lower reactivity.[54]

**On the Mechanism of the Zinc Site.** The second issue that we approach in this study is the mechanism of thiolate alkylation. For complexes **1**−**4**, we have explored the potential free-energy surface for the three reaction mechanisms envisaged in the literature. Our data reflect a huge difference of behavior between models **1** and **2** and models **3** and **4**, with each reactivity being predominantly influenced by the electronic composition of the zinc ligands. For the neutral models **1** and **2** displaying a $[ZnNS_3]^0$ core, the favored alkylation goes through an associative $S_N2$ mechanism, whereas complexes **3** and **4** with a $[ZnNS_3]^{2-}$ dianionic core follow a dissociative $S_N2$ pathway. The difference between both models lies indeed in the dissociation energy of **1** and **3** (or **2** and **4**).

Because of the high dissociation energy for a neutral core, especially in the gas phase or in nonpolar media, the associative mechanism is the most competitive even if the unreachable free thiolate would be more reactive than the zinc-complexed thiolate. Among the two associative pathways, the $S_N2$-type transition state is lower in energy than the four-center one, indicating a nucleophilic reactivity. This is consistent with a previous study showing that the experimental reactivity of neutral zinc complexes toward MeI closely follows that predicted from the nucleophilicity of the zinc-bound thiolate measured as the energy of the highest occupied molecular orbital.[48]

On the contrary, the electronically rich complexes **3** and **4** will undergo preferentially dissociation, because the zinc−thiolate interaction is weak, and will thus react as free dissociated thiolates. Even if the zinc-bound thiolate is more reactive in **3** and **4** than in **1** and **2**, the associative $S_N2$ transition state, preferred from **1** and **2**, seems very unlikely to form, as shown by the lower energy of the dissociative $S_N2$ transition state.

These results, reflecting a mechanistic difference that depends on the electronic environment around the zinc center, allow us to clarify the diverse conclusions reported until now in the literature about the associative or dissociative aspect of the mechanism. Based on NMR study, the alkylation of $Zn(SPh)_4^{2-}$ by phosphotriesters was consistent with a dissociative pathway, leading to decoordination of thiolate from zinc before reaction.[29] On the contrary, numerous complexes show the retention of thiolate coordination to zinc before alkylation.[39,43,48,51,61] These differences in the mechanism may be explained by the difference in the net charge of the complexes, with the former being dianionic like **3** and **4**, whereas all of the latter are neutral like **1** and **2**.

All zinc enzyme active sites showing a reactivity toward the alkylating agent possess a global electronic charge of −1 or −2.[12] From our results, we can postulate that dianionic active sites such as those of the DNA repair protein Ada or of the cobalamin-dependent methionine synthase react through a dissociative pathway. For monoanionic active sites like protein farnesyl transferase or cobalamin-independent methionine synthase, we anticipate an intermediate situation where both mechanisms are possible, depending on more subtle factors like the protein hydrogen-bond network. This is consistent with the proposed associative transition state in the case of protein farnesyl transferase.[63] It should be noticed that the protonation states of $Zn(Cys)_4$ and $Zn(Cys)_3(His)$ cores are still a matter of debate. If these active sites include respectively two and one additional proton to achieve neutrality,[67,68] an associative mechanism would be preferred in all cases.

The intramolecular NH···S hydrogen bond does not influence the detailed mechanism followed by **2** and **4** compared to **1** and **3**, respectively. Even if for **2**, compared to **1**, the dissociative mechanism is slightly easier (39.7 vs 40.9 kcal/mol, respectively) and the associative $S_N2$ mechanism is slightly more difficult (26.9 vs 26.5 kcal/mol, respectively), the lower free-energy pathway is still the associative one. We cannot exclude, however, that in some

cases an intramolecular hydrogen bond may induce an inversion of the most competitive pathway or at least lead to a situation where both pathways can occur. The recent study of the reactivity of a $[ZnS_4]^0$ complex including an intramolecular hydrogen bond suggests a dissociative mechanism based on the isotope effect even if DFT calculations cannot definitely exclude the associative mechanism.[57] It is possible that the borderline situation described above applies in this case.

Model reactions with complexes including a neutral core indicate that the thioether, produced in the zinc coordination sphere, dissociates from the metal. The zinc keeps, however, its tetrahedral environment by coordinating an iodide.[51] A comparison of the relative energies of **1-INT5** and **1-PROD** ($\Delta G_{water} = -14.6$ kcal/mol) is consistent with this result. This is due to the weak interaction energy between the cationic $[H(pz^H)Bt^{Me}]Zn$ core and the thioether as reflected by a long Zn−S bond length (2.407 Å) and a weak dissociation energy (19.9 kcal/mol in the gas phase). We even notice that the inclusion of solvent effect leads to an exothermic dissociation by 1.4 kcal/mol. This trend is conserved and quantitatively slightly accentuated in the presence of an intramolecular NH···S hydrogen bond. In the case of a dianionic core, the Zn−thioether bond is still longer (2.734 and 2.806 Å for **3-INT5** and **4-INT5**, respectively), thus leading to its easy dissociation. Furthermore, in water, we found that iodide coordination to the $[H(pz^H)Bt^{2-}]Zn$ fragment is endothermic for **3** and **4**. This shows that the anionic $[ZnS_2N]^-$ does not bind strongly any of the available ligands. This is consistent with an experimental EXAFS study on protein farnesyl transferase indicating that the thioether is not tightly coordinated to the zinc.[91] A recent theoretical study on the same enzyme confirms this aspect by showing that the thioether dissociation from zinc applies with a small activation energy and is endothermic.[92] However, although weak, this interaction may be observed if surrounding hydrogen bonds hold the substrate as in cobalamin-independent methionine synthase[93] or even be significant if the thioether product belongs to the active site as in the DNA repair protein Ada.[17,18]

(91) Tobin, D. A.; Pickett, J. S.; Hartman, H. L.; Fierke, C. A.; Penner-Hahn, J. E. *J. Am. Chem. Soc.* **2003**, *125*, 9962–9969.
(92) Sousa, S. F.; Fernandes, P. A.; Ramos, M. J. *J. Comput. Chem.* **2007**, *28*, 1160–1168.
(93) Ferrer, J.-L.; Ravanel, S.; Robert, M.; Dumas, R. *J. Biol. Chem.* **2004**, *276*, 44235–44238.

## Conclusion

Using several biomimetic complexes, models of thiolate alkylating zinc enzymes, we have examined their reactivity and their reaction mechanism against methyl iodide. In accordance with experimental results, we find that intramolecular N−H···S hydrogen bonding reduces the nucleophilicity of the thiolate. Furthermore, we show that the net electronic charge of the complex plays a significant role not only in its reactivity but especially in the mechanism of thiolate alkylation. The mechanism of zinc-mediated alkyl group transfer to thiols has been subjected to controversy both in model systems and in the enzymes. Three types of pathways have been proposed: a dissociative $S_N2$ mechanism with a zinc-dissociated thiolate serving as a nucleophile or an associative mechanism, either a $\sigma$-bond metathesis or an $S_N2$ with direct alkylation on the zinc-bound thiolate. We have demonstrated that an $S_N2$ mechanism is followed in all cases, either with an associative or a dissociative character for $[ZnS_3N]^0$ or $[ZnS_3N]^{2-}$ cores, respectively. This agrees with the experimental results and explains the opposite data obtained with neutral complexes compared to those with $Zn(SPh_4)^{2-}$. All of the zinc enzyme active sites showing alkyl transfer activity have at least a −1 net charge, based on the hypothesis that zinc-bound cysteines are deprotonated. For dianionic active sites, we conclude that the dissociative $S_N2$ should be the preferred pathway. For monoanionic cases, we anticipate an intermediate situation where both $S_N2$ mechanisms are possible, depending on more subtle factors like the protein hydrogen-bond network. If some zinc-bound thiolates are protonated, leading to a neutral active site, a associative mechanism will be favored.

**Acknowledgment.** We are grateful to the Centre National de la Recherche Scientifique (CNRS) and Ecole Polytechnique for financial support. We also thank the Institut du Développement et des Ressources en Informatique Scientifique (IDRIS; Grant 0543) and the Centre Informatique National de l'Enseignement Supérieur (CINES; Grant dcm2335) for computational resources.

**Supporting Information Available:** Cartesian coordinates and absolute electronic, gas-phase, and solvation free energies for all compounds. This material is available free of charge via the Internet at http://pubs.acs.org.

IC800697S